

Transient effects in wavelength add-drop multiplexer chains

I. Roudas, J. L. Jackel, D. H. Richards, N. Antoniadis, and J. E. Baran

I. Roudas, J. L. Jackel, and J. E. Baran are with Bellcore, 331 Newman Springs Rd., Red Bank, NJ 07701-5699, USA

Corresponding author: I. Roudas, Tel: (732)758-3313, Email: roudas@bellcore.com

D. H. Richards is with the City College of New York, Department of Electrical Engineering, NY 10031

N. Antoniadis is with Columbia University, Dept. of EE, 530 W 120th st., New York, NY 10027, USA

Introduction – Servo-controlled attenuators are used within the network elements of multiwavelength optical networks as power equalizers to compensate for the interchannel power variations due to the non-flat gain of Erbium-doped fiber amplifiers (EDFAs) and due to the fact that signals do not originate at the same point [1].

Network reconfiguration, failures, protection switching, etc. may cause abrupt changes of the power levels at the input of the servo-controlled attenuators. Depending on their design, servo-controlled attenuators can exhibit transient oscillations before reaching the equilibrium. Transient oscillations caused by power variations of one wavelength channel can be coupled to other wavelength channels due to the cross-saturation effect of the EDFAs. This mechanism is responsible for sustained power fluctuations observed experimentally in large scale networks with closed loops [2].

This paper presents a theoretical study of the transient power fluctuations of wavelength add-drop multiplexer chains caused by the dynamic interaction of servo-controlled attenuators and saturated EDFAs. A generalized theoretical model of the servo-controlled attenuators is derived and validated experimentally. Using this model, it is shown that the network transient response depends on the magnitude of the initial optical power perturbation, the speed of servo-controlled attenuators, the design of EDFAs, the network topology, and the add/drop scenario. Elimination of the coupling of transients between wavelength channels can be achieved using gain-clamped EDFAs or fast servo-controlled attenuators.

Servo-controlled attenuator model – Servo-controlled attenuators can be based on a variety of different designs. An exhaustive study of servo-controlled attenuator circuitries is beyond the scope of this paper. A generalized model that captures the essential features of the servo-controlled attenuator's behavior is assumed (Fig. 1).

The model is composed of an optical tap (TAP), a photodetector (P), a lowpass electronic filter (LPF), a comparator (CMP), a control mechanism (CM), and an optical attenuator [i.e. multiplier by $a(t)$]. When the input signal enters the servo-controlled attenuator, its power $P_i(t)$ is reduced by $a(t)$. A small portion of the output light is tapped and detected by a photodiode. The photodiode is followed by a lowpass filter that eliminates fast power variations by averaging over a duration τ . The signal at the output of the lowpass filter is compared with a reference power value P_r . The resulting error signal $e(t)$ is used to drive the attenuator through a control mechanism. For simulation purposes, the control mechanism can be represented by a multiplier (K) and an integrator (INT). This representation stems from the (arbitrary) assumption that the rate of change of the attenuation is a linear function of the error signal. The attenuation $a(t)$ can be described by $da(t)/dt = Ke(t)$, where K is a proportionality constant related to the speed of the attenuator. The above relationship can be rewritten in the more eloquent integral form $a(t) = \int_{-\infty}^t Ke(t')dt'$ which indicates that only when there is a non-zero error signal the value of the attenuation changes. In the absence of error signal, the servo-controlled attenuator maintains its previous value. The ends of the attenuation range are set by an upper and a lower limit parameters. When the integration result would otherwise exceed the upper limit or fall below the lower limit, the output is set equal to the upper-limit or lower-limit value.

Validation of the servo-controlled attenuator model – The step response of the generalized servo-controlled attenuator described above can be derived analytically when the lowpass filter is modeled as a finite time integrator with impulse response duration τ . In the latter case, the attenuation is described by a delay-differential equation which can be solved in closed form by considering successive time segments of duration τ and using Laplace transform techniques [3]. However, the analytical solution is cumbersome and simulation is necessary for the study of servo-controlled attenuator cascades or more complex network topologies.

Simulation shows that the step response of the generalized servo-controlled attenuator depends on the choice of the servo-controlled attenuator design parameters K , τ , and on the level of the input power jump.

Different combinations of the above quantities result in completely different behavior of the output power, that varies from exponentially damped to underdamped oscillations and clipping when the ends of the attenuation range are reached.

To illustrate the above points and test the validity of the model, measurements of the step response of a commercially available opto-mechanical servo-controlled attenuator are compared with simulation results.

Fig. 2 shows the measured (solid line) and the simulated (broken line) optical power at the output of the servo-controlled attenuator when the input power is suddenly increased by 3 dB at the time instant $t = 350$ ms. The overshoot of the output power is instantaneous. After the overshoot, the output power oscillates and eventually reaches a constant reference value. Although not visible in the time scale of the graph, it is found that the oscillation frequency decreases gradually during the step as the output power approaches the equilibrium value. Despite the simplicity of the theoretical model, there is a good qualitative agreement between theory and experiment. In the following the servo-controlled attenuator model is applied to the study of the transient response of multiwavelength optical networks.

Network model – In Fig. 3, the architecture of a simplified Wavelength Add-Drop Multiplexer (WADM) [1] is shown. The depicted WADM consists of two EDFAs (1), a demultiplexer (DMUX) (2), 2x2 optical switches for signal adding/dropping (3), servo-controlled attenuators for power equalization (4), and a multiplexer (MUX) (5).

Fig. 4 shows a chain of three such WADMs in cascade. Without loss of generality, it is assumed that only two wavelength channels are present. Both wavelength channels (denoted in the figure by λ_1, λ_2 respectively) are added in the first WADM. In the third WADM, wavelength channel 1 is dropped and another optical signal is added at the same wavelength. It is assumed that all wavelength channels are added at $t \rightarrow -\infty$ so that the network has reached equilibrium at $t \rightarrow 0^-$. It is also assumed that the power of wavelength channel 1 in the first WADM is increased suddenly by 3 dB at the instant $t = 0$. Simulations are used to investigate if power variations in that channel can be transferred to other channels.

Wavelength-domain simulation [4] is used to evaluate the performance of the topology shown in Fig. 4. The numerical values of the parameters used in the simulation are the following: Fiber spans between WADMs are assumed to have 21 dB flat attenuation (i.e. the fiber length is assumed 60 km with attenuation 0.35 dB/km). A single-stage EDFA model is used that provides approximately flat gain 21.7 dB/channel when the input power is -8 dBm/channel. The MUX/DMUX are hierarchical blocks composed of two elementary filters in parallel. The elementary filters are approximated by ideal rectangular filters with Full Width at Half Maximum (FWHM) of 100 GHz. The insertion loss of a MUX/DMUX pair is 10 dB per channel. The optical 2x2 switches are assumed to have 3 dB insertion loss/channel and negligible optical crosstalk. The servo-controlled attenuators are automatically adjusted to equalize the signal power at a reference value -8 dBm per channel at the input of the power booster EDFA in each WADM. The insertion loss of the servo-controlled attenuators is 2 dB. They are operated at 6 dB additional attenuation. The servo-controlled attenuator design parameters K, τ are chosen so that the output power decays exponentially for the assumed input perturbation rather than showing the underdamped oscillations of Fig. 2. The servo-controlled attenuators are assumed to respond much slower to changes in input power than the EDFA gain. Therefore, in the simulation a static EDFA model is used [5]. In reality the output power variations consist of a fast component due to EDFA response that decays in a time scale of the order of milisecond and a slow component due to the attenuator response that is assumed to last for several tens of miliseconds. The results do not include the fast component due to EDFA response. Transmission impairments are neglected.

Results and Discussion – Fig. 5 (a), (b) show the output powers for wavelength channels 1, 2 respectively at the output of the three WADMs. For $t < 0$ the optical power at the output of all WADMs is constant 13.7 dBm/channel. At the instant $t = 0$, the optical power at the output of the servo-controlled attenuator corresponding to wavelength channel 1 in the first WADM instantaneously increases and then decays exponentially to its initial value. After the WDM signal passes through the power booster EDFA of the first WADM, power variations in channel 1 induce complementary power variations in the channel 2 (curves 1). The effect is more pronounced at the output of the second WADM (curves 2). In the third WADM, channel 1 is dropped and a new channel at the same wavelength is added. The new channel is physically disjoint from channel 1. However, the power transient of channel 1 is transferred to the new

channel through the complementary power transients acquired by channel 2 in the first two WADMs (curves 3). In the above graphs, the propagation delay of the power perturbation between WADMs is not taken into account.

These results indicate that the cascade of N WADMs is equivalent to $2N$ oscillators (i.e. servo-controlled attenuators) coupled at $2N$ nodes (i.e. EDFAs). This system has modes of oscillation which can be excited through different add/drop scenarios. The result is a progressive wave (i.e. power perturbation) that propagates from the beginning to the end of the chain. If closed loops exist, standing waves can be formed depending on the propagation delay. Therefore, the servo-controlled attenuators oscillators and the EDFAs must be properly designed in order for the oscillations to be completely damped.

To avoid coupling of power variations from one channel to other channels, gain-clamped amplifiers can be used [2]. Preliminary simulations show that the coupling between wavelength channels will be negligible or very small in this case. Only the wavelength channel that experienced the initial perturbation is affected. For this channel the perturbation evolves as it propagates through a transparent chain of cascaded network elements.

Another solution for avoiding coupling of power variations from one channel to other channels is to use servo-controlled attenuators which respond much faster to changes in input power than the EDFA gain. Again, only the wavelength channel that experienced the initial perturbation is affected. The study of the above remedies will be part of future simulations.

This work was performed as a part of the MONET consortium under DARPA funding agreement MDA 972-95-3-0027.

References

- [1] N. Antoniadis et al., *IEEE Phot. Tech. Lett.*, vol. 9, pp. 1274-1276, Sep. 1997.
- [2] S. Yoo et al., in *Optical Fiber Communication Conference (OFC)*, no. paper WJ2, (San Jose, CA), Feb. 1998.
- [3] A. C. Tsoi, in *Recent theoretical developments in control* (M. J. Gregson, ed.), (University of Leicester), pp. 67-127, Institute of Mathematics and its Applications, Sept. 1976.
- [4] I. Roudas et al., submitted to *J. Lightwave Technol.*
- [5] C. R. Giles and E. Desurvire, *J. Lightwave Technol.*, vol. 9, pp. 271-283, Feb. 1991.

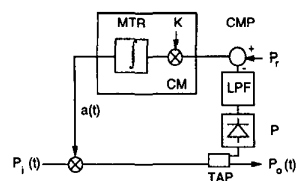


Figure 1: General model of the servo-controlled attenuator.

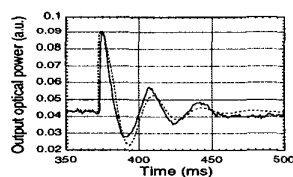


Figure 2: Step response of a commercial servo-controlled attenuator (Solid line: experiment; broken line: simulation).

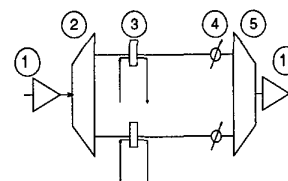


Figure 3: Block diagram of a Wavelength Add-Drop Multiplexer.

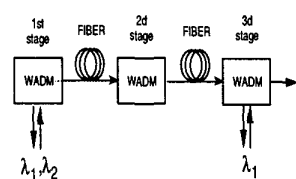


Figure 4: Block diagram of a chain of Wavelength Add-Drop Multiplexers.

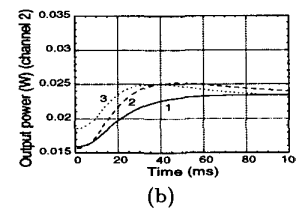
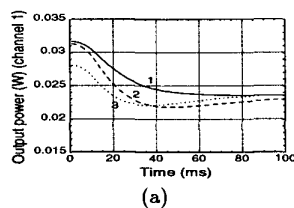


Figure 5: Optical power at the output of the i -th WADM of the chain ($i=1, 2, 3$) (a) channel 1; (b) channel 2.